Glia maturation factor modulates β-amyloid-induced glial activation, inflammatory cytokine/chemokine production and neuronal damage

Asgar Zaheer[1,2], **Smita Zaheer**[3], **Ramasamy Thangavel**[2], **Yanghong Wu**[2], **Shailendra K. Sahu**[2,4], and **Baoli Yang**[3]

[1]*Veterans Affair Medical Center, Iowa City, IA*

[2]*Division of Neurochemistry and Neurobiology, Department of Neurology, University of Iowa, Iowa City, IA 52242*

[3]*Department of Obstetric and Gynecology, University of Iowa, Iowa City, IA 52242*

[4]*Department of Neurosurgery, University of Iowa, Iowa City, IA 52242*

Abstract

Glia maturation factor (GMF), discovered and characterized in our laboratory, is a highly conserved protein primarily localized in mammalian central nervous system. Previously we demonstrated that GMF is required in the induced production of proinflammatory cytokines and chemokines in brain cells. We now report that ventricular infusion of human amyloid beta peptide1-42 (Aβ1-42) in mouse brain caused glial activation and large increases in the levels of GMF as well as induction of inflammatory cytokine/chemokine known for launching the neuro inflammatory cascade in Alzheimer's disease (AD). To test the hypothesis that GMF is involved in the pathogenesis of AD, we infused Aβ1-42 in the brain of GMF-deficient (GMF-KO) mice, recently prepared in our laboratory. GMF-deficient mice showed reduced glial activation and significantly suppressed proinflammatory cytokine/chemokine production following Aβ infusion compared to wild type (Wt) mice. The decrease in glial activation in the GMF-KO mice is also associated with significant reduction in Aβ induced loss of pre-synaptic marker, synaptophysin, and post-synaptic density protein-95 (PSD 95). We also examined the potential relationship between GMF or lack of it with learning and memory using the T-maze, Y-maze, and water maze, hippocampal-dependent spatial memory tasks. Our results show that memory retention was improved in GMF-KO mice compared to Wt controls following Aβ infusion. Diminution of these Aβ1-42 effects in primary cultures of GMF-KO astrocyte and microglia were reversed by reconstituted expression of GMF. Taken together, our results indicate a novel mediatory role of GMF in neuro-inflammatory pathway of Aβ and its pro-inflammatory functions.

Keywords

Address correspondence to: Asgar Zaheer, Department of Neurology, The University of Iowa, 200 Hawkins Drive, Iowa City, IA 52242, Tel. 319-335-8529; Fax 319-335-6821; E-Mail: asgar-zaheer@uiowa.edu.

1. Introduction

Alzheimer's disease (AD) is a neuronal disease characterized by the accumulation of amyloid plaques and neurofibrillary tangles (NFT) leading to neuro degeneration. The reactive astrocytes and microglia play a critical role in escalating inflammatory responses that contribute significantly to the pathogenesis of AD. Such inflammatory response involves the production of several inflammatory mediators, including proinflammatory cytokines/ chemokines that are associated with the stress-activated signal transduction pathways. In the central nervous system microglia plays an important role in immune surveillance, host defense, and tissue repair. Under adverse and certain pathological conditions, resting microglia undergo an activation process characterized by increased production of proinflammatory mediators, including deleterious free radicals, that are capable of initiating or exacerbating the progression of AD pathology (Giulian et al. 1995; Meda et al. 2001; Minagar et al. 2002). The hallmark of AD pathology is the presence of great number of reactive astrocytes and activated microglia near neuritic plaques that are composed of β-amyloid aggregates. The precise mechanism of neuro degeneration by glial activation in AD is not clear.

Expression of high levels of proinflammatory cytokines and chemokines in the CNS are thought to contribute to neuronal injury leading to cytokine-induced cognitive impairment (Wilson et al. 2002). The activated microglia and astrocytes produce a variety of proinflammatory molecules such as tumor necrosis factor-α (TNF-α), interferon-γ (IFN-γ), interleukin-1 beta (IL-1β), IL-12 and granulocyte macrophage-colony stimulating factor (GM-CSF). Studies in transgenic and knockout mice now provide strong and direct evidence of individual cytokine, such as TNF-α, IL-6, IFN-γ (Hull et al. 1996; Liu et al. 1998; Samoilova et al. 1998; Hamilton et al. 2002), involvement in CNS inflammation. Increased levels of several chemokines including CXCR3, IP-10, and MIP-1β were found in AD (Bradt et al. 1998; Xia et al. 2000; Xia and Hyman 2002). These chemokines are potent chemoattractant for activated T cells and regulate their migration into CNS and thus the subsequent inflammation in brain.

A large body of evidence suggests that prolonged glial activation contributes to CNS inflammation leading to neuro degeneration. A better understanding of the processes of neuro inflammation and neuro degeneration relevant to AD progression is critical. We previously demonstrated that GMF is a prominent mediator of inflammatory signal transduction in CNS leading to the death of neuronal cells (Zaheer et al. 2007b; Zaheer et al. 2007a). In the current studies, we investigate the role of GMF in the pathogenesis and aggravation of AD. As the population of the United States ages rapidly, this neurodegenerative disease is reaching to an epidemic proportion. No curative measures have yet been found. The study of the pro-inflammatory role of GMF promises to contribute to the development of new therapeutic strategies for this devastating illness.

2. Results

2.1. Aβ 1-42 infusion into the mouse brain induce glial activation, GMF and inflammatory cytokine/chemokine production

We induced AD-relevant pathologies by intracerebroventricular injection of human Aβ1-42 in GMF-KO and Wt mice as described in Methods. These mice show robust neuro inflammation, Aβ plaques, and neuronal damage (Frautschy et al. 1996;Frautschy et al. 2001;Craft et al. 2004). The expression of GMF in the brain at day 7, 14 and 21 following Aβ1-42 injections were analyzed by Western blot analysis using specific anti-GMF antibody. Results in Fig. 1 show significant increases in the amount of GMF at days 14 and 21 in the brain of mice receiving Aβ1-42. The mRNA levels of GMF and inflammatory cytokines/

chemokines, TNF-γ, IL-1β, IFN-γ, MCP-1 and IP-10 as estimated by real-time PCR in the brain of mice, increased significantly with time during 7, 14 and 21 days post injections (Fig. 2). The maximum increased values of GMF, TNF-γ, IL-1β, IFN-γ, MCP-1 and IP-10 at 21 days after Aβ injections were 7.2 ± 0.4, 4.7 ± 0.6, 4.8 ± 0.6, 5.3 ± 0.9, 5.6 ± 1.0.and 6.6 ± 0.9 fold, respectively relative to the baseline value in saline (vehicle) injected mice. The Aβ1-42 injection induced a significant increase in GMF levels along with inflammatory cytokines and chemokines in the brain.

2.2 Significant suppression of Aβ-induced activation of astrocytes and microglia in GMF-KO mice

We studied the role of GMF in Aβ-induced neuro inflammation *in vivo* using GMF-KO mice. Intracerebroventricular infusion of Aβ1-42 in GMF-KO and control Wt mice was performed for four weeks using a micro-osmotic pump (Alzet #1002, 75 ng/h oligomeric Aβ1-42), essentially as described (Craft et al. 2004). At post-operative day 28, activated GFAP-positive astrocytes and F4/80-positive microglia in the hippocampus, as detected by immunohistochemical analysis, were low, 6 and 23 in vehicle infused control Wt mice but increased to large values of 56 for activated astrocytes and 94 for activated microglia in Aβ-infused Wt mice. On the other hand, these activations by Aβ were muted in GMF-KO mice. Compared to the Wt mice, identical Aβ infusion in GMF-KO produced significantly lower, 30 and 47 values of activated astrocytes and microglia, respectively (Fig. 3A & B). Reduced numbers of activated astrocytes and activated microglia were visible in Aβ-infused GMF-KO mice compared to Wt controls (Fig. 3C & D).

2.3. Significant suppression of Aβ-induced proinflammatory cytokines in GMF-KO mice

We detected significant reduction in the levels of Aβ-induced pro inflammatory IL-1β and TNF-α in GMF-KO mice compared to Wt mice (Fig. 4). The levels of IL-1β and TNF-α cytokines, measured by quantitative ELISA in the hippocampal extracts of Aβ-infused Wt mice were 167.5 ± 4.6 pg/mg and 127.7 ± 5.6 pg/mg protein, respectively. But the respective values were significantly reduced to 49.1 ± 3.1 pg/mg and 27.7 ± 5.6 pg/mg of protein in Aβ-infused GMF-KO mice. The extracts of vehicle (saline)-infused Wt and GMF-KO mice had very low, 32.4 ± 1.0 and 27.7 ± 3.6 pg of IL-1β per mg of protein in addition to TNF-α at levels of 17.9 ± 6.7 and 13.7 pg /mg of protein. The concentrations of the two cytokines in these vehicle controls did not differ significantly between Wt and GMF-KO mice.

2.4. Reduced expression of Aβ-induced inflammatory cytokine/chemokine in GMF-KO glial cells

We study the role of GMF in Aβ-induced expression of proinflammatory cytokine and chemokine in primary cultures of glial cells. Cells were treated with 15 µM Aβ1-42 (oligomeric and fibrillar) for 24 h and levels of cytokine/chemokine were measured by ELISA. To quantitate responses to oligomeric and fibrillar forms of Aβ1-42, we allowed Aβ1-42 to form oligomers or fibrils as described by Kayed et al. (Kayed et al. 2003). We found significant reduction in the expressions of IL-1β and MCP-1 in GMF-KO astrocytes (Fig. 5 A & B) and microglia (Fig. 5C & D) compared to Wt glial cells. The increased levels of cytokines/ chemokines were returned in GMF-KO cells reconstituted to over express GMF with an adenoviral GMF construct. Fibrillar Aβ was far less effective than Oligomeric Aβ in inducing IL-1β and MCP-1 expressions in these cells.

2.5. Significant suppression of Aβ-induced neuronal loss in GMF-KO mice

Significant reduction in the loss of the pre-synaptic marker, synaptophysin, and post-synaptic density protein-95 (PSD-95) was detected in GMF-KO mice infused with Aβ1-42. Western

blot analysis (Fig. 6) of hippocampal extracts showed a significant reduction in these neuronal markers in Aβ-infused mice compared to vehicle-infused GMF-KO mice.

2.6 Elevated levels of GMF in the hippocampus, frontal cortex, and entorhinal cortex of Aβ1-42-infused mice

A representative example of a brain section through the cerebral cortex of Aβ1-42-infused and Veh-infused (via micro-pump for28 days) mouse subjected to immunocytochemistry for fibrillary β-amyloid plaques is shown in Fig. 7. The immunocytochemistry clearly demonstrates the presence of numerous β-amyloid plaques in the Aβ1-42-infused mouse brain. Quantitative ELISA was performed to determine levels of GMF in microdissected hippocampus, frontal cortex, entorhinal cortex and cerebellum tissue of Aβ1-42-infused and Veh-infused mice (via micro-pump for28 days). The hippocampus, frontal cortex and entorhinal cortex regions were chosen because these regions are implicated in the earliest stages of AD disease. The presence of high concentration of GMF was detected in hippocampus, frontal cortex, and entorhinal cortex regions (Fig. 8), but not in cerebellum of the Aβ1-42-infused mice.

2.7. Significantly improved memory retention in GMF-KO mice

GMF-KO mice were created by homologous recombination, with more than 80% (exons 2–6 out of a total of 7) of the amino acid coding sequence deleted, as described earlier (Zaheer et al, 2004). The result was confirmed by the total absence of the GMF protein on these animals. GMF-KO mice were maintained by backcross breeding to C57BL/6. Mice between 5 and 6 months old were used for this study. Absence of GMF gene was non-lethal to the mice, which developed to maturity showing no difference in weight and no gross morphological abnormality. Routine observation, handling and checking failed to detect gross behavioral differences between the knockout and the wild-type animals, including free locomotion and exploration, tail movement, body posture, paw grip, muscle strength, muscle tone, spontaneous urination and defecation. When tested with the elevated "plus" maze, both groups crossed the intersection the same number of times, and spent the same fraction of time in the enclosed area (a measure of fear), indicating no difference in activity level and anxiety, respectively. Equal numbers of males and females were included, since preliminary data showed no difference with respect to sex. GMF-KO and Wt groups were matched for age and sex for each behavioral test.

Wt and GMF-KO mice following Aβ infusion (via micro-pump for28 days) were tested for simple position discrimination with a T-maze using positive reinforcement. Results in Fig. 9 show that the control vehicle-infused Wt and GMF-KO mice exhibited a parallel learning response over time with no overall significant difference. Where as there was a significant difference in the results between Wt and GMF-KO mice following Aβ infusion.

The Y maze test, an index of hippocampal-dependent spatial memory, revealed significant differences between Wt and GMF-KO mice following Aβ infusion. In these experiments mice have to learn which of the two arms of the Y-maze is baited with a food reward. Results (Fig. 10) show that the memory retention was about the same in control wild type and GMF-KO mice that were not infused with Aβ but the memory retention retarded drastically in Wt from 85% of mice entering into correct arm in vehicle control to 45% at 14 days and from 80% to 25% at 21 days after Aβ infusion. Whereas, Aβ caused only slight reductions in the memory retention in GMF-KO mice, from 90 % correct arm entries in vehicle control to 78% at 14 days and from 85% in control to 70% at 21 days after Aβ infusion. The memory retention in GMF-KO mice remained significantly higher compared to Wt mice (Fig. 10) following identical Aβ infusions.

We examined the ability of Wt and GMF-KO mice to acquire and retain spatial information in the Morris water maze task as indicative of learning and memory functions. The trials were performed after 28 days of Aβ infusion via a micro-pump. When tested for spatial memory in Morris water maze, both control and knockout groups learned to locate the hidden platform with the same latency, suggesting no difference in spatial learning (Fig. 11). The $A\beta_{1-42}$ infusion caused a decline of spatial learning and memory in Wt and GMF-KO, as indicated by increased latencies to find the platform during the trials. GMF-KO mice were less susceptible to the cognitive deficits observed following $A\beta_{1-42}$ infusion compared to Wt mice (Fig. 11). A control trial for swimming speed conducted before the experiment revealed that the two groups had equal swimming ability. A probe trial after the experiment confirmed that both groups remembered the location of the platform.

Thus, our results demonstrate, for the first time, that the cognitive deficits induced by $A\beta_{1-42}$ in mice can be modulated by GMF.

3. Discussion

Alzheimer's disease is the most common form of dementia among older people, affecting 4 million Americans and over 12 million individuals worldwide. The etiology of AD remains unknown and there is no definite treatment yet available. The pathology of AD is characterized by neuritic plaques containing aggregates of β-amyloid peptide, neurofibrillary tangles composed of hyper phosphorylated microtubule-associated protein tau, degenerating neurons, and abundance of reactive astrocytes and activated microglia. Although it is commonly accepted that amyloid plaques and neurofibrillary tangles are the main causative factors for neuronal death, other factors also play important role in aggravating the severity of the disease. These include reactive astrocytes and activated microglia (and macrophages), production of pro-inflammatory cytokines, chemokines and other agents toxic to the neurons. The neurotoxic mechanisms may also involve free radicals such as reactive oxygen species/reactive nitrogen species and the transcription factor NF-kB. How the inflammatory reaction in the central nervous system contributes to neuronal death in AD is currently unclear.

Research efforts in recent years on GMF, a highly conserved brain-specific protein, isolated, sequenced and cloned in our laboratory, have demonstrated pro-inflammatory functions for GMF. It has been established in our lab that overexpression of GMF in astrocytes leads to activation of microglia through secretion of granulocyte-macrophage-colony stimulating factor (Zaheer et al. 2002; Zaheer et al. 2007b). Using DNA microarray analysis, we found that GMF activates a host of genes in the nervous system related to immuno/inflammatory activity, including tumor necrosis factor-α (TNF-α), GM-CSF, interleukin 1-beta (IL-1β), MIP-1 β, complement protein C1q, class II major histocompatibility complex (MHC) proteins, 12-lipoxygenase and chemokine CX3C. All of these are known to be associated with the pathophysiology of neurodegenerative disorders such as AD. We also reported the stimulation of p38 mitogen activated protein kinase (p38 MAPK) pathway and nuclear factor kappa B (NF-kB) by GMF in primary astrocyte cultures (Lim and Zaheer 1996; Zaheer and Lim 1996, 1998; Lim et al. 2000; Zaheer et al. 2001; Zaheer et al. 2007b). Recently, we have reported (Zaheer et al. 2007a; Zaheer et al. 2007b) that the overexpression of GMF in astrocytes leads to the destruction of primary oligodendrocytes and neurons by interactions between highly purified cultures of astrocytes, microglia, oligodendrocytes and neurons. We infected astrocytes with a replication-defective adenovirus carrying the GMF cDNA. The overexpression of GMF caused the activation of p38 MAP kinase and transcription factor NF-κB, as well as the induction of GM-CSF mRNA and protein in astrocytes. Small interfering RNA-mediated GMF knockdown completely blocked the GMF-dependent activation of p38 MAPK, NF-κB, and enhanced expression of GM-CSF by astrocytes. Inhibition of p38 MAPK or NF-κB by specific inhibitors prevented GM-CSF production. The cell-free conditioned

medium from overexpressing GMF astrocytes contained enough GM-CSF for enhanced production and secretion of TNF-α, IL-1β, IL-6, and IFN-γ-IP10 by microglia. Presence of these inflammatory cytokines in the conditioned medium from microglia efficiently destroyed oligodendrocytes and neurons in culture. These results suggested that GMF-induced production of GM-CSF in astrocytes is dependent on p38 MAPK and NF-κB activation. The GM-CSF-dependent expression and secretion of inflammatory cytokines, TNF-α, IL-1β, IL-6, and IFN-γ-IP10, is cytotoxic to oligodendrocytes, the myelin-forming cells in the central nervous system, and as well as neurons. Our results suggested a novel pathway of GMF initiated cytotoxicity of brain cells, and implicates its involvement in inflammatory diseases such as AD and MS. Additionally, induced production of the proinflammatory cytokines were diminished in GMF-knockout (GMF-KO) mice *in vivo* and in brain cells from GMF-KO mice *in vitro*. Forced expression of GMF in these cells from GMF-KO mice restored the copious production of the same proinflammatory cytokines leading to neurotoxicity *in vitro*. Based on GMF's ability to activate microglia and induce several well-established pro-inflammatory mediators, we hypothesize that GMF is involved in the pathogenesis of AD. We carried out experiments to test this hypothesis using GMF-KO mice, recently prepared in our laboratory.

The major finding of this study is the demonstration that GMF-KO show reduced neuro inflammation, reduced neuronal damage, and improved memory retention following Aβ infusion compared to control Wt mice. The reduction in Aβ-induced neuro inflammation was demonstrated by measurement of astrocyte and microglia activation as well as induction of pro inflammatory cytokines/chemokines believed to play a critical role in the neuro inflammatory cascade in AD. The decrease in glial activation in the GMF-KO mice is also associated with reduced neuronal and synaptic damage observed following Aβ infusion, suggesting that GMF overexpression leads to neuro inflammation that potentiates the neurotoxic effects of Aβ. These data provide further support to our hypothesis that increased levels of GMF in the AD brain contributes to neuro inflammatory and neuro degenerative processes that are detrimental to brain function. In the present study, we also determined for the first time, the effect of GMF or lack of it in mice by performing learning and memory tests involving higher and specific brain function. The hippocampal-dependent spatial learning in the Morris water task included training to locate a hidden escape platform followed by measuring the amount of time taken to locate and the distance traveled to the escape platform. We also measured the quadrant search time and the number of time a subject crossed the exact location of the platform that has been removed from its original place (probe trial). Other learning and memory tests included a T-maze and a Y-maze for spontaneous alternation. The Y-maze test with only one arm baited with a food reward throughout the experiment is considered to be hippocampus dependent. Our results demonstrate for the first time that the cognitive deficits induced by $Aβ_{1-42}$ in mice can be modulated by GMF. Our results are in agreement with the other reports implicating neuro inflammation and the cytotoxic lesions of the hippocampus in severe memory impairments in mouse model of AD (Frautschy et al. 1996; Frautschy et al. 2001; Craft et al. 2004; Craft et al. 2005c; Craft et al. 2005b; Craft et al. 2005a; Hu et al. 2005; Deacon et al. 2002; Reisel et al. 2002). The overall results suggest that targeting GMF and its neuro inflammatory signal pathway represents an attractive strategy for development of new therapeutic intervention in AD.

4. Experimental procedures

4.1. Reagents

Adenovirus constructs were prepared at the University of Iowa Gene Transfer Vector Core as described earlier (Davidson et al. 1993; Lim et al. 1998; Zaheer et al. 2007b), using a replication-defective adenovirus (serotype 5) vector. The constructs contained either a full-length GMF cDNA (Ad5CMVGMF), or a cytoplasmic lacZ cDNA (Ad5CMVcytolacZ).

CT-11 was a monoclonal antibody (IgG1) against a synthetic peptide corresponding to the C-terminal 11 amino acid residues of GMF and was affinity-purified with protein-A. PCR primers were synthesized at Integrated DNA Technologies (Coralville, IA). Trizol® reagent (Cat# 15596-026), ThermoScript™ RT-PCR system (Cat #11146-016) for first-strand cDNA synthesis were purchased from Invitrogen Corporation, CA. ELISA kits for mouse TNF-α (Cat # KMC3011), IL-1β (Cat # KMC0011), and MCP-1 (Cat # KMC0061) were obtained from Biosource International, Anti-F4/80 and mouse anti-GFAP (Cat # MAB360) were from Chemicon, CA.

4.2. Cell Culture

Primary cultures of astrocytes and microglia were prepared essentially as described previously by us (Zaheer et al. 2001; Zaheer et al. 2002; Zaheer et al. 2007b) and by others (Assouline et al. 1983; Delgado and Ganea 2003). Mixed glial culture were established from newborn mouse brain by trypsin dissociation and cultured for 8–10 days as previously described. Astrocytes were purified by differential attachment as follows. The mixed glial cells were sub-cultured by trypsinization and reseeding. Twenty minutes after plating, when approximately 2/3 of the cells (mainly astrocytes) have attached, the medium was changed to remove the floating and loose cells. The adhered cells were permitted to grow to a confluent monolayer. Cells were subcultured at least twice to achieve homogeneous monolayers of astrocytes. Astrocytes were grown in DMEM/F12 containing 5% fetal bovine serum (complete medium). Astrocyte cultures were >98% positive for glial fibrillary acidic, a specific marker for astrocytes. Microglia enriched cultures were obtained using the method of Giulian et al. (Giulian and Baker 1986; Giulian et al. 1986; Chao et al. 1993). Briefly, a mixed glial culture was subjected to shaking at 200 rpm on a gyratory shaker for 30 min. The detached cells (mainly microglia with few oligodendroglia) were reseeded in fresh culture flasks, and after 2 hours any contaminating oligodendrocyte progenitors were detached with Tris-buffered saline containing 1 mM EDTA. This procedure routinely provides a firmly attached homogeneous population of microglia. Microglia were cultured in DMEM/F12 containing 10% FBS. Over ninety five percent of such a preparation of microglial cell was found to be positive for anti-CD11b, a specific marker for these cells.

4.3. Overexpression of GMF in glial cells

Transient transfection experiments to overexpress GMF in primary cultures of glia were carried out as described earlier (Lim et al. 1998; Zaheer et al. 2007b). Replication-defective human adenovirus vector containing a full length GMF cDNA (GMF-V) or cytoplasmic lacZ cDNA (LacZ) at 10 MOI (multiplicity of infectivity) were added to cells in serum-free and antibiotic free DMEM/F12 medium for 4 h. At the end of infection period, cells were gently rinsed once and allowed to grow in the same medium. In mock-transfected controls, the above procedure was carried out in the absence of virus. The efficiency of infection was estimated to be over 95% as determined by X-gal staining.

4.4. Quantitative estimation of mRNA by real-time RT-PCR

Reverse transcription-polymerase chain reaction (RT-PCR) was carried out as described earlier (Zaheer et al. 1995a; Zaheer et al. 1995b; Zaheer et al. 2007b) in detail. For this purpose total RNA was isolated from cultured cells by the acid guanidinium thiocyanate-phenol-chloroform method (Chomczynski and Sacchi 1987), using the Trizol reagent. The primer pairs were selected to yield a single amplicon based on dissociation curves and analysis by acrylamide gel electrophoresis. The following oligonucleotide primers were used:

GMF, 5'-ACG CTG GGA GTA AGA ACA AGC T-3' and 5'-GGT CCT CGG TGT TTC TTA TTT CAA A-3'; TNF-α, 5'- CAT CTT CTC AAA ATT CGA GTG ACA A-3' and 5'-TGG GAG TAG ACA AGG TAC AAC CC-3'; IL-1β, 5'-CAA CCA ACA AGT GAT ATT

CTC CAT G-3' and 5'- GAT CCA CAC TCT CCA GCT GCA-3'; IP10, 5'- GCC GTC ATT TTC TGC CTC AT -3' and 5'- GCT TCC CTA TGG CCC TCA TT -3'; 18S, 5'- TAA GTC CCT GCC CTT TGT ACA CA-3' and 5'- GAT CCG AGG GCC TCA CTA AAC-3'. Real-time quantitative PCR was performed in a model ABI Prism 7000 sequence detection system. The thermal cycler parameters were as follows: hold for 2 min at 50°C and 10 min at 95°C for one cycle followed by amplification of cDNA for 40 cycles with melting for 15 s at 95°C and annealing and extension for 1 min at 60°C. The values were normalized using 18S rRNA as an endogenous internal standard (Livak and Schmittgen 2001).

4.5. Enzyme-linked immunosorbent assay (ELISA)

The analysis of TNF-α, IL-1β, and MCP-1 protein concentration was estimated by sandwich immuno-assay procedure as specified in the manufacturer's protocol (BioSources, CA). The concentration of cytokine was estimated from a standard curve generated with each run. The lower detection limits of these ELISA are in the range of 10–15 pg/ml. ELISA data are presented as mean values ± standard deviations and represent more than three independent experiments with similar results.

4.6. Western Immunoblotting

Cells and tissue were extracted with a lysis buffer consisting of 1% Triton X-100, 50 mM Tris-HCl (pH 7.5), 100 mM NaCl, 50 mM NaF, 0.1 mM sodium vanadate, 1 mM benzamidine, 1 mM PMSF, and 10 µg/ml each of aprotinin, leupeptin, chymostatin, pepstatin A and antipain. Equal amount of protein samples were separated on 4–20% gradient gels by SDS-polyacrylamide gel electrophoresis, and electroblotted onto nitrocellulose membranes. Protein blots were probed with specific primary antibodies (1:1000 v/v) and developed by using the appropriate secondary antibody conjugated to horseradish peroxidase (HRP) (1:2000 v/v).

4.7. Aβ infusion

We induced AD-relevant pathologies by intracerebroventricular injection of human amyloid-β peptide1-42 (Aβ1-42) in GMF-KO and Wt mouse brain essentially as described (Frautschy et al. 1996; Frautschy et al. 2001; Craft et al. 2004; Craft et al. 2005c; Craft et al. 2005b; Craft et al. 2005a; Hu et al. 2005). For this purpose, 1 ul of 1mg/ml solution of Aβ1-42 or vehicle (saline) was injected very slowly at 1 mm depth through a burr hole at 1 mm anterior and 1 mm lateral to the Bregma. The prolonged infusion of Aβ1-42 (100 ng/h) or vehicle (saline) in right lateral cerebral ventricle was performed at 6 µl/day for 28 days using a micro-osmotic pump (Alzet #2004) placed under skin and attached to a mouse brain cannula (Plastics One) implanted at stereotaxic coordinates, −1.0mm mediolateral, −0.5mm anteroposterior from Bregma and −1.5mm dorsal-ventral from skull (Craft et al., 2004). The surgery and slow intracerebral injection were performed in anesthetized mice and the animals were cared for in accordance with the guidelines approved by the IACUC and National Institutes of Health.

4.8. Histology

At each sampling time point, six mice in each group were anaesthetized and perfused with saline. One hemi brain was frozen for neurochemical analysis, and the other hemi brain was used for histopathological studies. The tissues were dehydrated and then embedded in paraffin. Free-floating immunohistochemical analysis was performed on 25 µm thick sections. Immuno-histochemical detection of activated astrocytes, as measured by GFAP-staining, and microglial activation, as measured by F4/80 immunoreactivity, was performed following Aβ1-42 infusion. GFAP-positive astrocytes and F4/80-positive microglia were counted in the hippocampus (three sections/mouse and 6 mice each group) essentially as described by Craft et al. (Craft et al. 2004).

4.9. T-maze

A T-maze was made of three arms, each 30 cm long, 6 cm wide, with sidewalls of 8 cm high. During acclimation, the food (reinforcer), consisting of a mixture of cookies, cheese, and cereal, was placed at the end of the two goal arms, readily accessible, and the mouse was placed in the starting arm and permitted to explore freely. The arm that the mouse less preferred to enter was chosen as the correct goal for that mouse throughout all the trials. During the test, food was place in both goal arms behind a visual barrier. A correct response was scored when the mouse passed the intersection, with all four paws in the correct arm, within a time of 30 s. Once in the correct arm, the mouse was rewarded with a nibble of the food by having the barrier removed. If the mouse entered the wrong arm or failed to enter either goal arm within 30 s, the trial was scored negative and the test was started over. Each mouse was given a session of 10 consecutive trials per day for 11 consecutive days. Mice were deprived of food (but not water) for 12 h before each session, and were permitted to access animal feed ad lib after the session. Simple position discrimination was used to test instrumental procedural learning, which is independent of hippocampal function.

4.10. Y-maze test

Behavioral testing in Y-maze was carried in 5–6 month old C57/BL6 Wt and GMF-KO at 7, 14, and 21 days after infusion with human $A\beta1$-42 or without (vehicle controls). The stem arm and the two arms forming the Y were 8 and 6 inch long, respectively, and diverged at a 45° angle from the stem arm. In this experiment, mice had to learn which of the two arms forming the Y was baited with food. During the experiment, only one of the two arms contained food. If the mouse entered into the correct arm containing food, one correct entry was recorded. If the mouse entered to the other arm with no food in it, one wrong entry was recorded. The mice were trained until they correctly entered into the food-containing arm 9 out of 10 continuous training trials. The mouse was allowed to eat the small piece of food. The mouse was allowed to enter the maze again for the next trial after cleaning of the arms. The Y-maze test was repeated 7 days after the first test. The percentage of correct arm entries in 6 trials was used to compare the memory.

4.11. Morris water maze

The maze was made of a circular pool 105 cm in diameter, 60 cm deep, with a water level of 40 cm. The water (15 °C) was made opaque by mixing with non-toxic Crayola paint. A hidden platform, 12 cm in diameter, was submerged 1 cm below the water surface. During each trial, the mouse was placed along the edge of the pool and allowed a maximum time of 60 s to locate the platform, which was placed in one of the four quadrants (N, E, S or W) of the pool. The platform location stayed the same for each animal, but the starting point differs from day to day. Animals within the same group were assigned different platform locations. Each mouse received one trial each day, for a total of 15 days. Permanent visual cues (star, moon, square, and triangle) were fixed on the walls of the room, at a height and distance clearly visible from the pool. A video camera was mounted above the pool to record the behavior of each animal. Morris water maze was used to measure spatial memory, which is a declarative learning dependent of hippocampal function.

4.12. Statistical analysis

Results presented as mean values ± standard deviations. Statistical significance was assessed with ANOVA followed by Tukey's procedure using SigmaStat software (SPP, Chicago, IL). A value of $p < 0.05$ was considered statistically significant. Statistical analyses of behavioral studies were performed in the Department of Biostatistics at the University of Iowa using a SAS software (Version 9.0, SAS Institute, 2003). Detailed procedures are included in figure legends.

Acknowledgments

References

Assouline JG, Bosch EP, Lim R. Purification of rat Schwann cells from cultures of peripheral nerve: an immunoselective method using surfaces coated with anti-immunoglobulin antibodies. Brain research 1983;277:389–392. [PubMed: 6605783]

Bradt BM, Kolb WP, Cooper NR. Complement-dependent proinflammatory properties of the Alzheimer's disease beta-peptide. J Exp Med 1998;188:431–438. [PubMed: 9687521]

Chao CC, Molitor TW, Hu S. Neuroprotective role of IL-4 against activated microglia. J Immunol 1993;151:1473–1481. [PubMed: 8335941]

Chomczynski P, Sacchi N. Single-step method of RNA isolation by acid guanidinium thiocyanate-phenol-chloroform extraction. Anal Biochem 1987;162:156–159. [PubMed: 2440339]

Craft JM, Watterson DM, Van Eldik LJ. Neuroinflammation: a potential therapeutic target. Expert opinion on therapeutic targets 2005a;9:887–900. [PubMed: 16185146]

Craft JM, Watterson DM, Frautschy SA, Van Eldik LJ. Aminopyridazines inhibit beta-amyloid-induced glial activation and neuronal damage in vivo. Neurobiol Aging 2004;25:1283–1292. [PubMed: 15465624]

Craft JM, Watterson DM, Marks A, Van Eldik LJ. Enhanced susceptibility of S-100B transgenic mice to neuroinflammation and neuronal dysfunction induced by intracerebroventricular infusion of human beta-amyloid. Glia 2005b;51:209–216. [PubMed: 15810011]

Craft JM, Watterson DM, Hirsch E, Van Eldik LJ. Interleukin 1 receptor antagonist knockout mice show enhanced microglial activation and neuronal damage induced by intracerebroventricular infusion of human beta-amyloid. Journal of neuroinflammation 2005c;2:15. [PubMed: 15967035]

Davidson BL, Allen ED, Kozarsky KF, Wilson JM, Roessler BJ. A model system for in vivo gene transfer into the central nervous system using an adenoviral vector. Nat Genet 1993;3:219–223. [PubMed: 8387378]

Deacon RM, Bannerman DM, Kirby BP, Croucher A, Rawlins JN. Effects of cytotoxic hippocampal lesions in mice on a cognitive test battery. Behavioural brain research 2002;133:57–68. [PubMed: 12048174]

Delgado M, Ganea D. Vasoactive intestinal peptide prevents activated microglia-induced neurodegeneration under inflammatory conditions: potential therapeutic role in brain trauma. Faseb J 2003;17:1922–1924. [PubMed: 12923064]

Frautschy SA, Yang F, Calderon L, Cole GM. Rodent models of Alzheimer's disease: rat A beta infusion approaches to amyloid deposits. Neurobiol Aging 1996;17:311–321. [PubMed: 8744413]

Frautschy SA, Hu W, Kim P, Miller SA, Chu T, Harris-White ME, Cole GM. Phenolic anti-inflammatory antioxidant reversal of Abeta-induced cognitive deficits and neuropathology. Neurobiol Aging 2001;22:993–1005. [PubMed: 11755008]

Giulian D, Baker TJ. Characterization of ameboid microglia isolated from developing mammalian brain. J Neurosci 1986;6:2163–2178. [PubMed: 3018187]

Giulian D, Baker TJ, Shih LC, Lachman LB. Interleukin 1 of the central nervous system is produced by ameboid microglia. J Exp Med 1986;164:594–604. [PubMed: 3487617]

Giulian D, Haverkamp LJ, Li J, Karshin WL, Yu J, Tom D, Li X, Kirkpatrick JB. Senile plaques stimulate microglia to release a neurotoxin found in Alzheimer brain. Neurochem Int 1995;27:119–137. [PubMed: 7655344]

Hamilton NH, Banyer JL, Hapel AJ, Mahalingam S, Ramsay AJ, Ramshaw IA, Thomson SA. IFN-gamma regulates murine interferon-inducible T cell alpha chemokine (I-TAC) expression in dendritic cell lines and during experimental autoimmune encephalomyelitis (EAE). Scand J Immunol 2002;55:171–177. [PubMed: 11896933]

Hu W, Ralay Ranaivo H, Craft JM, Van Eldik LJ, Watterson DM. Validation of the neuroinflammation cycle as a drug discovery target using integrative chemical biology and lead compound development with an Alzheimer's disease-related mouse model. Current Alzheimer research 2005;2:197–205. [PubMed: 15974919]

Hull M, Strauss S, Berger M, Volk B, Bauer J. The participation of interleukin-6, a stress-inducible cytokine, in the pathogenesis of Alzheimer's disease. Behavioural brain research 1996;78:37–41. [PubMed: 8793035]

Kayed R, Head E, Thompson JL, McIntire TM, Milton SC, Cotman CW, Glabe CG. Common structure of soluble amyloid oligomers implies common mechanism of pathogenesis. Science (New York, N.Y 2003;300:486–489.

Lim R, Zaheer A. In vitro enhancement of p38 mitogen-activated protein kinase activity by phosphorylated glia maturation factor. J Biol Chem 1996;271:22953–22956. [PubMed: 8798479]

Lim R, Zaheer A, Kraakevik JA, Darby CJ, Oberley LW. Overexpression of glia maturation factor in C6 cells promotes differentiation and activates superoxide dismutase. Neurochem Res 1998;23:1445–1451. [PubMed: 9814556]

Lim R, Zaheer A, Yorek MA, Darby CJ, Oberley LW. Activation of nuclear factor-kappaB in C6 rat glioma cells after transfection with glia maturation factor. J Neurochem 2000;74:596–602. [PubMed: 10646510]

Liu J, Marino MW, Wong G, Grail D, Dunn A, Bettadapura J, Slavin AJ, Old L, Bernard CC. TNF is a potent anti-inflammatory cytokine in autoimmune-mediated demyelination. Nat Med 1998;4:78–83. [PubMed: 9427610]

Livak KJ, Schmittgen TD. Analysis of relative gene expression data using real-time quantitative PCR and the 2(-Delta Delta C(T)) Method. Methods 2001;25:402–408. [PubMed: 11846609]

Meda L, Baron P, Scarlato G. Glial activation in Alzheimer's disease: the role of Abeta and its associated proteins. Neurobiol Aging 2001;22:885–893. [PubMed: 11754995]

Minagar A, Shapshak P, Fujimura R, Ownby R, Heyes M, Eisdorfer C. The role of macrophage/microglia and astrocytes in the pathogenesis of three neurologic disorders: HIV-associated dementia, Alzheimer disease, and multiple sclerosis. J Neurol Sci 2002;202:13–23. [PubMed: 12220687]

Reisel D, Bannerman DM, Schmitt WB, Deacon RM, Flint J, Borchardt T, Seeburg PH, Rawlins JN. Spatial memory dissociations in mice lacking GluR1. Nature neuroscience 2002;5:868–873.

Samoilova EB, Horton JL, Hilliard B, Liu TS, Chen Y. IL-6-deficient mice are resistant to experimental autoimmune encephalomyelitis: roles of IL-6 in the activation and differentiation of autoreactive T cells. J Immunol 1998;161:6480–6486. [PubMed: 9862671]

Wilson CJ, Finch CE, Cohen HJ. Cytokines and cognition--the case for a head-to-toe inflammatory paradigm. J Am Geriatr Soc 2002;50:2041–2056. [PubMed: 12473019]

Xia M, Hyman BT. GROalpha/KC, a chemokine receptor CXCR2 ligand, can be a potent trigger for neuronal ERK1/2 and PI-3 kinase pathways and for tau hyperphosphorylation-a role in Alzheimer's disease? Neuroimmunol 2002;122:55–64.

Xia MQ, Bacskai BJ, Knowles RB, Qin SX, Hyman BT. Expression of the chemokine receptor CXCR3 on neurons and the elevated expression of its ligand IP-10 in reactive astrocytes: in vitro ERK1/2 activation and role in Alzheimer's disease. J Neuroimmunol 2000;108:227–235. [PubMed: 10900358]

Zaheer A, Lim R. In vitro inhibition of MAP kinase (ERK1/ERK2) activity by phosphorylated glia maturation factor (GMF). Biochemistry 1996;35:6283–6288. [PubMed: 8639570]

Zaheer A, Lim R. Overexpression of glia maturation factor (GMF) in PC12 pheochromocytoma cells activates p38 MAP kinase, MAPKAP kinase-2, and tyrosine hydroxylase. Biochem Biophys Res Commun 1998;250:278–282. [PubMed: 9753620]

Zaheer A, Zhong W, Lim R. Expression of mRNAs of multiple growth factors and receptors by neuronal cell lines: detection with RT-PCR. Neurochem Res 1995a;20:1457–1463. [PubMed: 8789608]

Zaheer A, Yorek MA, Lim R. Effects of glia maturation factor overexpression in primary astrocytes on MAP kinase activation, transcription factor activation, and neurotrophin secretion. Neurochem Res 2001;26:1293–1299. [PubMed: 11885780]

Zaheer A, Mathur SN, Lim R. Overexpression of glia maturation factor in astrocytes leads to immune activation of microglia through secretion of granulocyte-macrophage- colony stimulating factor. Biochem Biophys Res Commun 2002;294:238–244. [PubMed: 12051700]

Zaheer A, Zhong W, Uc EY, Moser DR, Lim R. Expression of mRNAs of multiple growth factors and receptors by astrocytes and glioma cells: detection with reverse transcription-polymerase chain reaction. Cell Mol Neurobiol 1995b;15:221–237. [PubMed: 8590453]

Zaheer A, Zaheer S, Sahu SK, Yang B, Lim R. Reduced severity of experimental autoimmune encephalomyelitis in GMF-deficient mice. Neurochem Res 2007a;32:39–47. [PubMed: 17151915]

Zaheer A, Zaheer S, Sahu SK, Knight S, Khosravi H, Mathur SN, Lim R. A novel role of glia maturation factor: induction of granulocyte-macrophage colony-stimulating factor and pro-inflammatory cytokines. J Neurochem 2007b;101:364–376. [PubMed: 17250654]
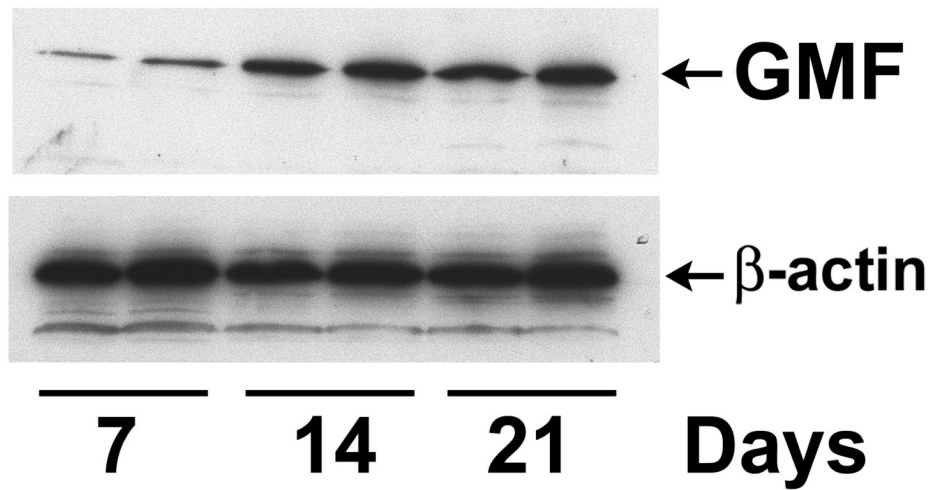
Fig. 1.
Immunoblot showing expression of GMF in Aβ1-42 injected mice brains. Two mice in each group at day 7, 14, and 21 post injections were analyzed by Western blot using an affinity-purified monoclonal antibody (CT-11) against a synthetic peptide corresponding to the C-terminal 11 amino acid residues of GMF. β-actin was included for sample control. The figure is representing three independent experiments.
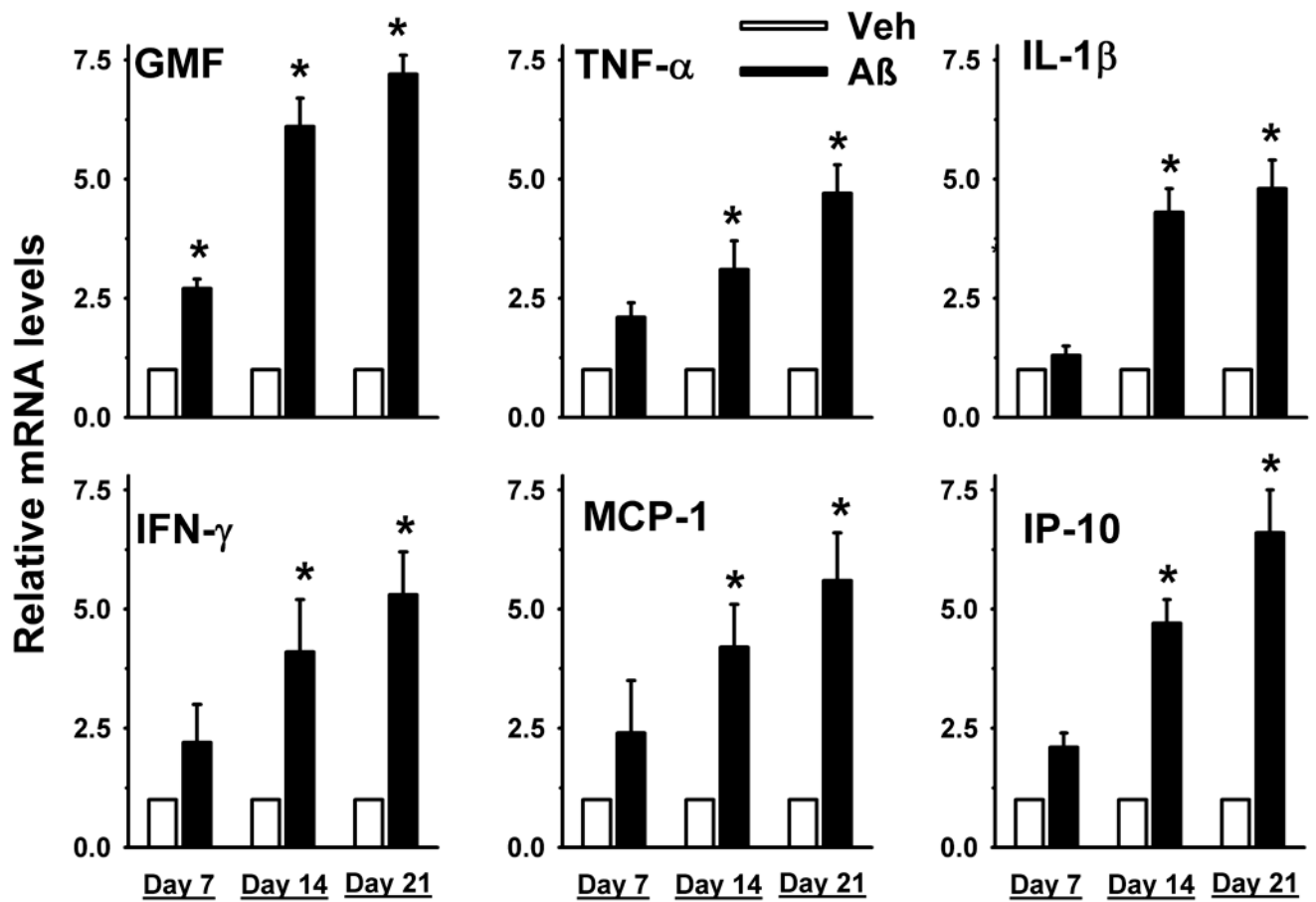
Fig. 2.
Significantly increased levels of GMF and inflammatory cytokines/chemokines in the brain of
Aβ1-42 injected mice. The mRNA expression levels were determined on days 7, 14, and 21
p.i. by real-time RT-PCR. Data represent the mean ± S.D. from three independent experiments.
* Vehical-infused Vs Aβ-infused. (* = p< 0.05)

(A) Astrocytes
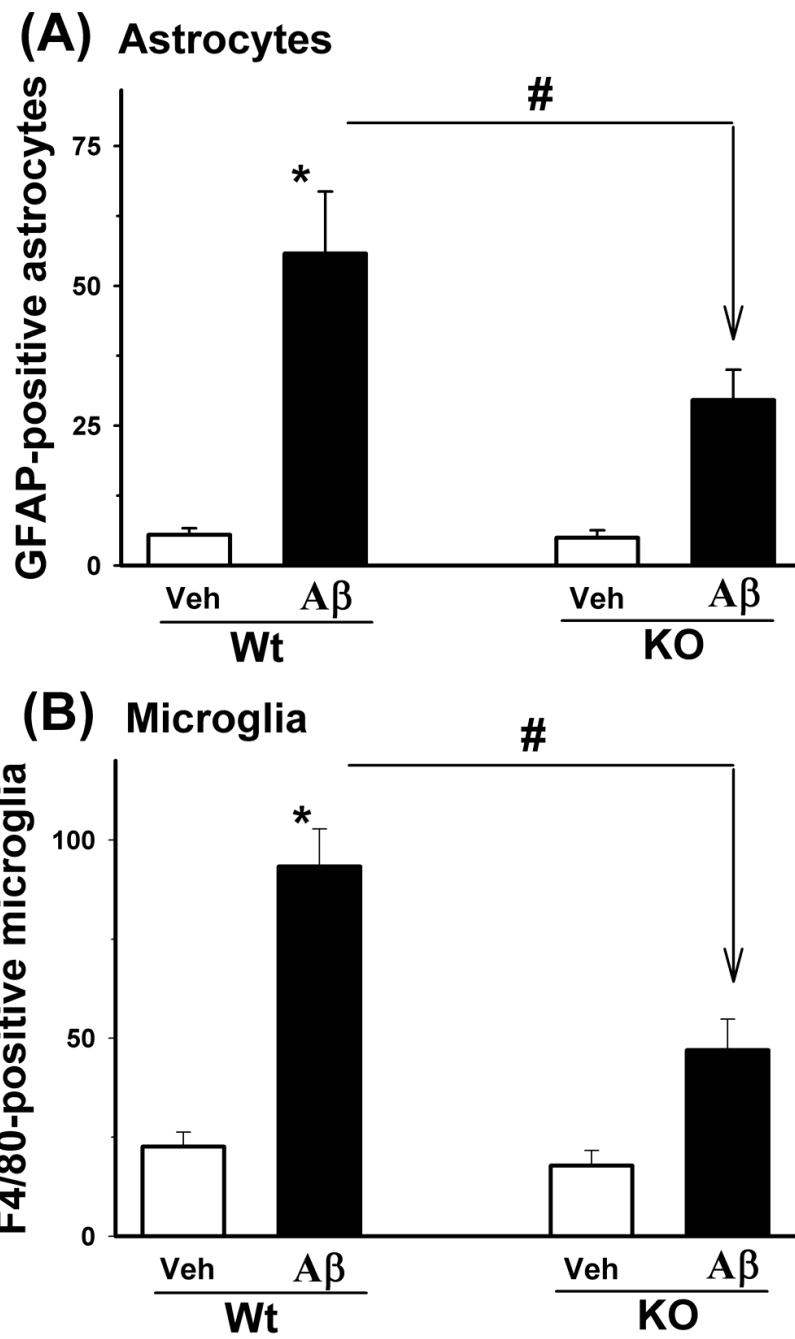
(B) Microglia

C-Astrocytes
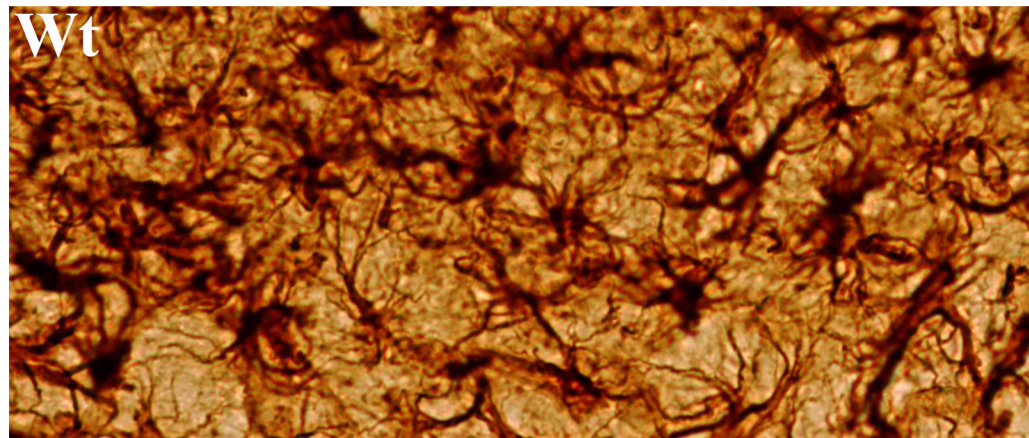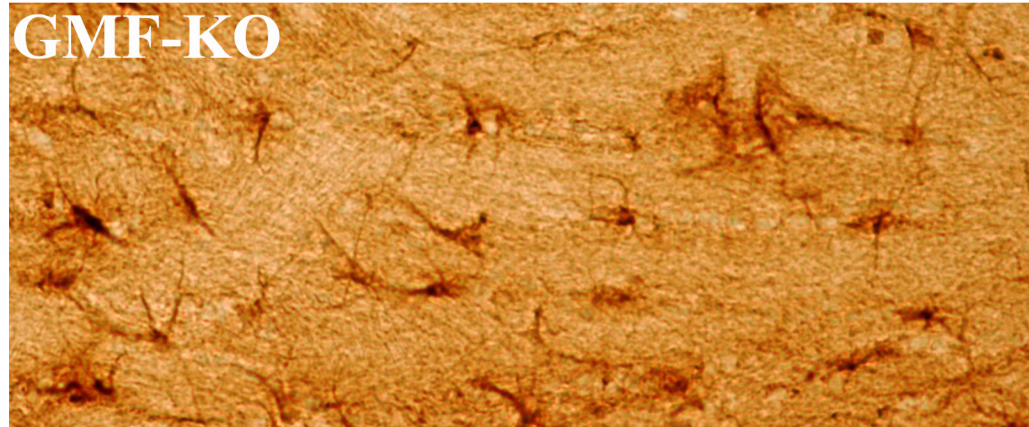
D-Microglia
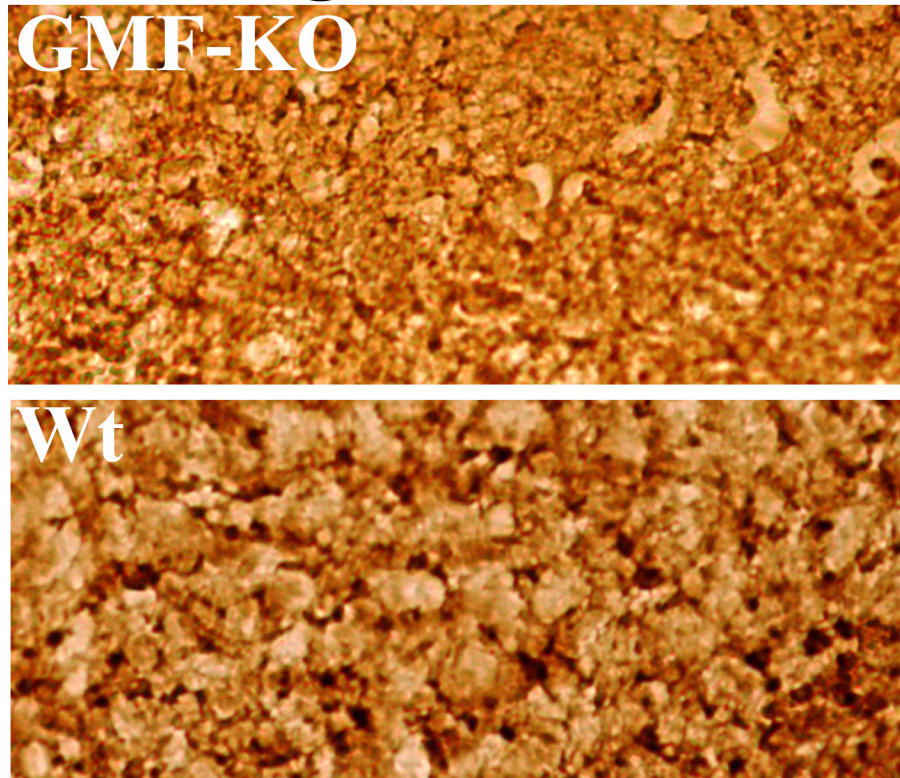
Fig. 3.
Significant suppression of glial cell activation in GMF-KO mice infused with amyloid beta. Intracerebro-ventricular infusion of Aβ1-42 was for four weeks using a micro-osmotic pump (Alzet). At post-operative day 28, activated GFAP-positive astrocytes **(A)** and F4/80-positive microglia **(B)** in the hippocampus were measured (n= 5 mice per group). Representative micrographs of GFAP-positive astrocytes **(C)** and F4/80-positive microglia **(D)** in Aβ-infused GMF-KO and Wt are shown (X40 magnification). * Vehical-infused Vs Aβ-infused. # Aβ-infused Wt Vs Aβ-infused GMF-KO. (p< 0.05)
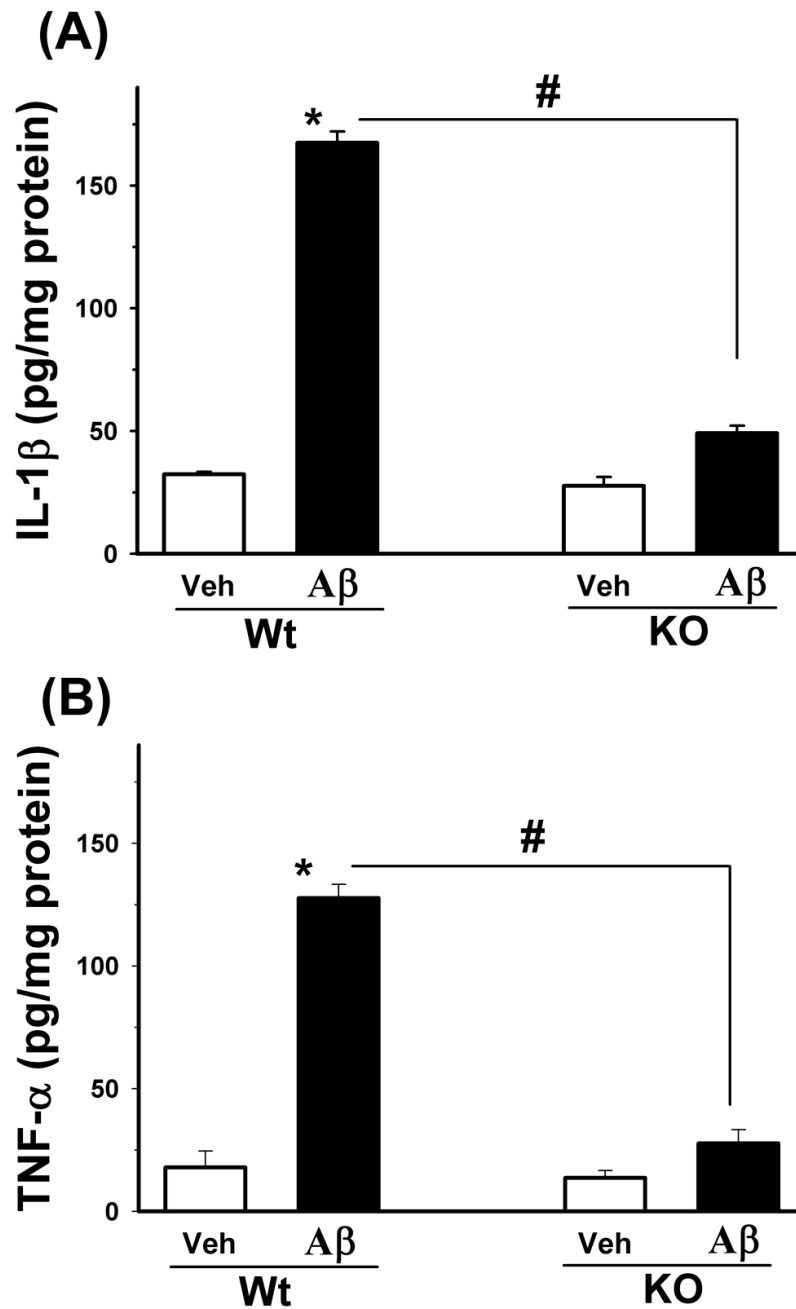
Fig. 4.
Significant suppression of the increase in proinflammatory cytokines IL-1β **(A)** and TNF-α **(B)** in GMF-KO mice infused with Aβ1-42. Cytokines were measured by ELISA in hippocampal extracts. (p< 0.05)
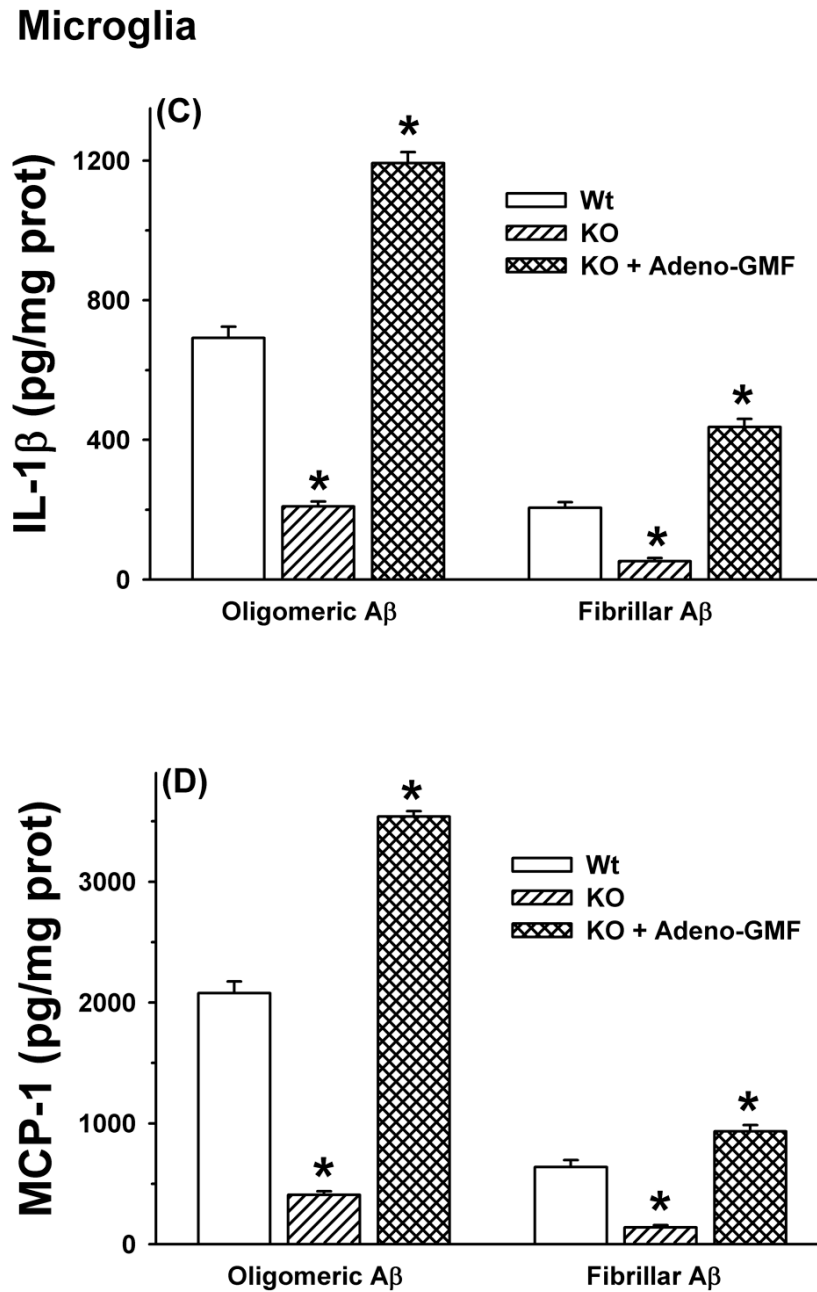
Astrocyte
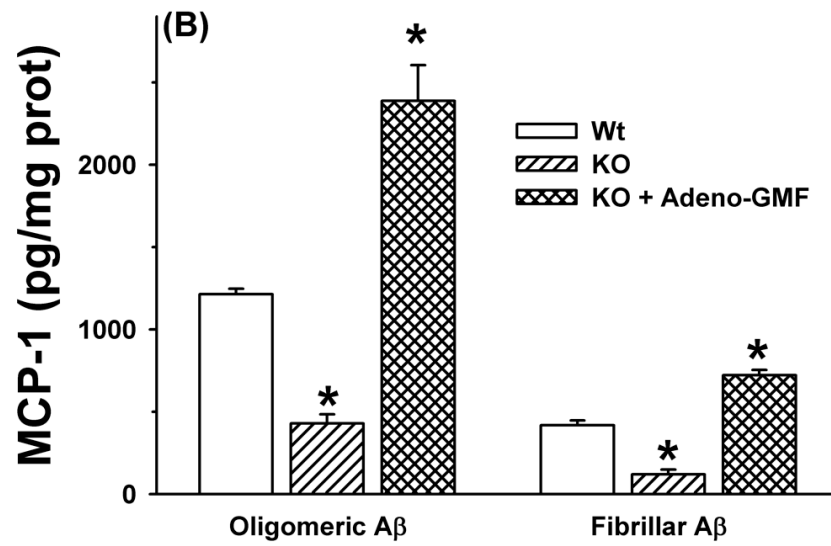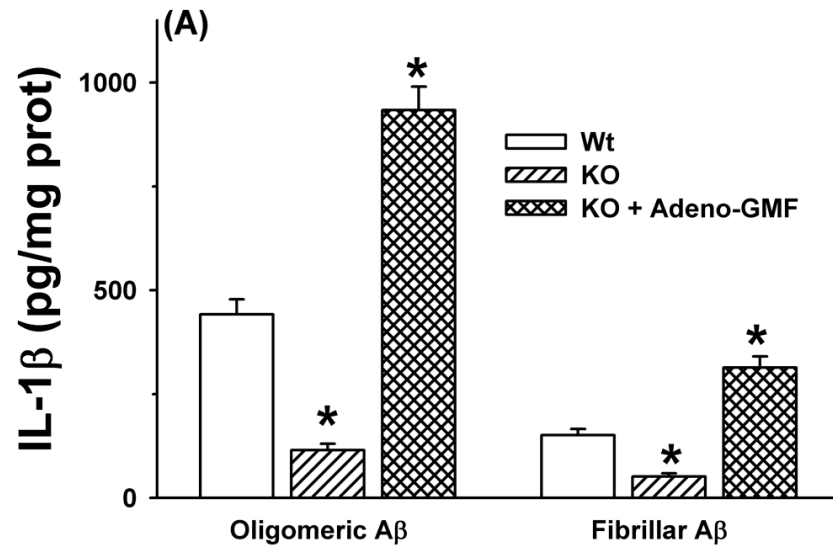
Microglia

Fig. 5.
Reduced expressions of inflammatory cytokine/chemokine in primary cultures of GMF-KO astrocytes (**A & B**) and microglia (**C & D**) compared to Wt glial cells and return of increased levels in GMF-KO cells reconstituted to over express GMF with an adenoviral GMF construct. Cells were treated with 15 µM Aβ1-42 (oligomeric and fibrillar) for 24 h and levels of cytokine/chemokine were measured by ELISA. Note significant difference between oligomeric and fibrillar Aβ. (p< 0.05)

(A) Synaptophysin   (B) PSD-95

Synpt.

β-actin

Veh Aβ Veh Aβ
Wt   KO

PSD-95

β-actin

Veh Aβ Veh Aβ
Wt   KO
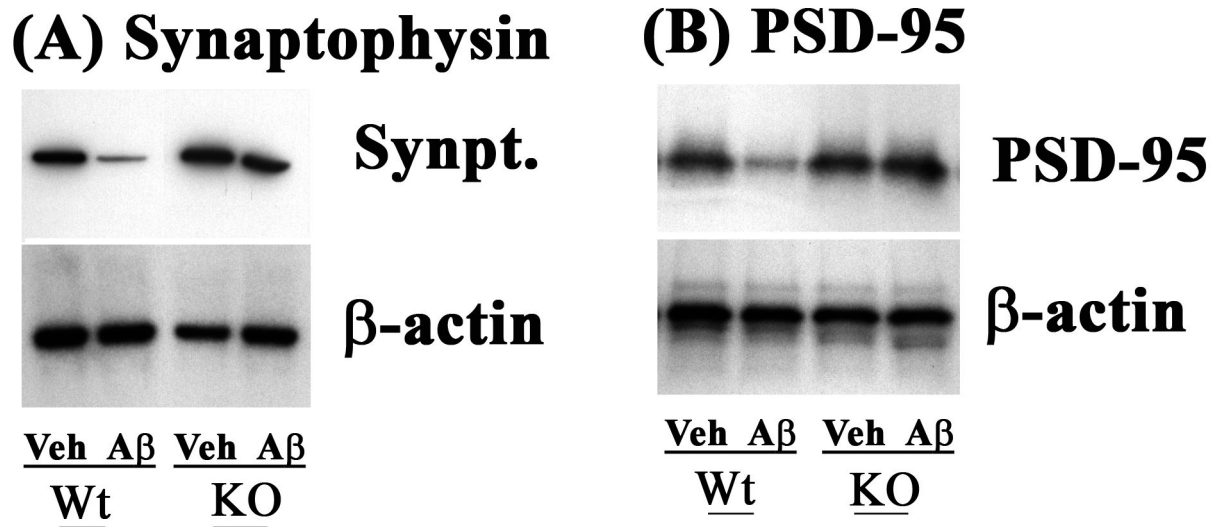
Fig. 6.
Significant reduction in the loss of synaptic markers, synaptophysin and post-synaptic density protein-95 (PSD-95) in GMF-KO mice infused with Aβ1-42. Western blot analysis of presynaptic protein **(A)** and post-synaptic protein **(B)** showed significant reduction in hippocampal extracts of Aβ-infused GMF-KO mice compared to Aβ-infused Wt mice. The results shown are representative and were repeated a minimum of three times.
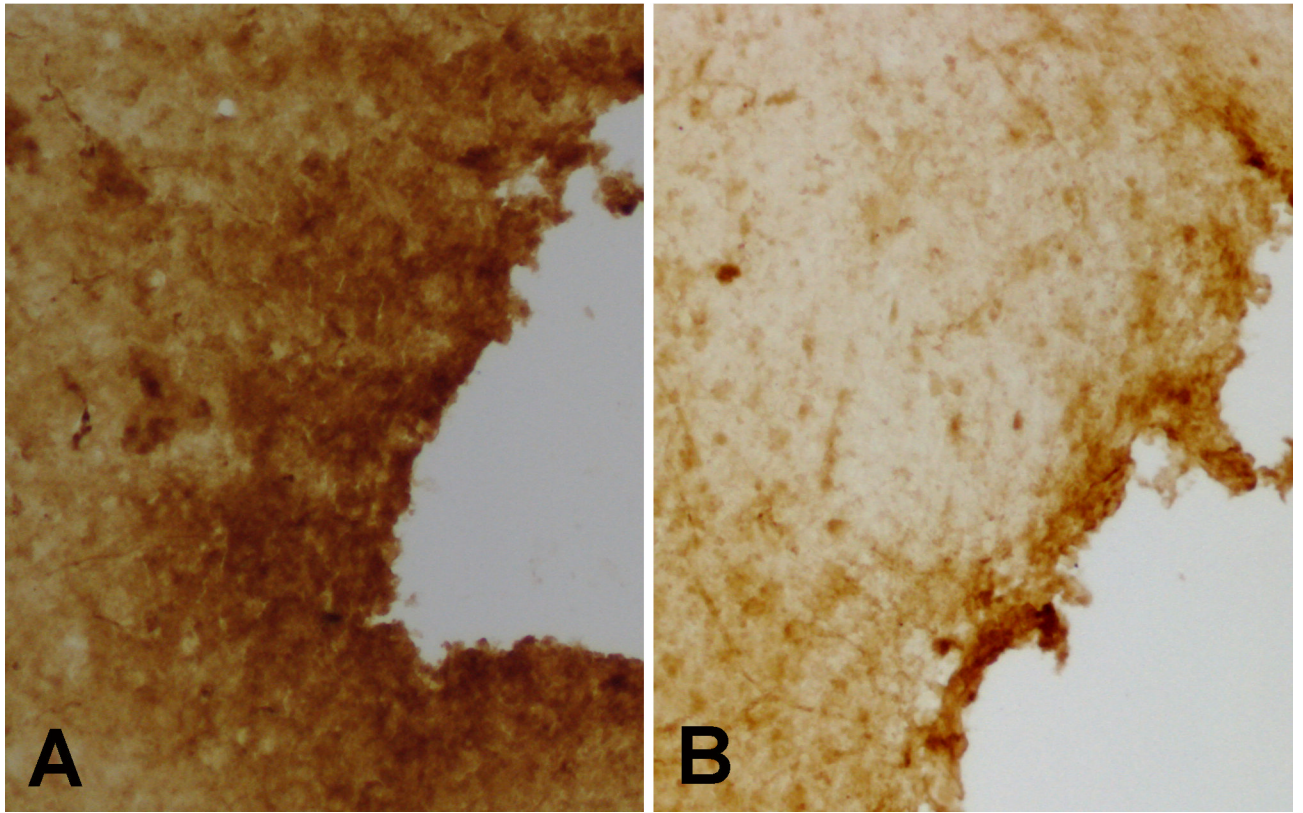
Fig. 7.
Representative micrograph of cerebral cortex from Aβ-infused or Veh-infused mice (via micro-pump for28 days). Note numerous β-amyloid plaques in Aβ-infused mice (A) as compared to Veh-infused mice (B). X40 magnifications.
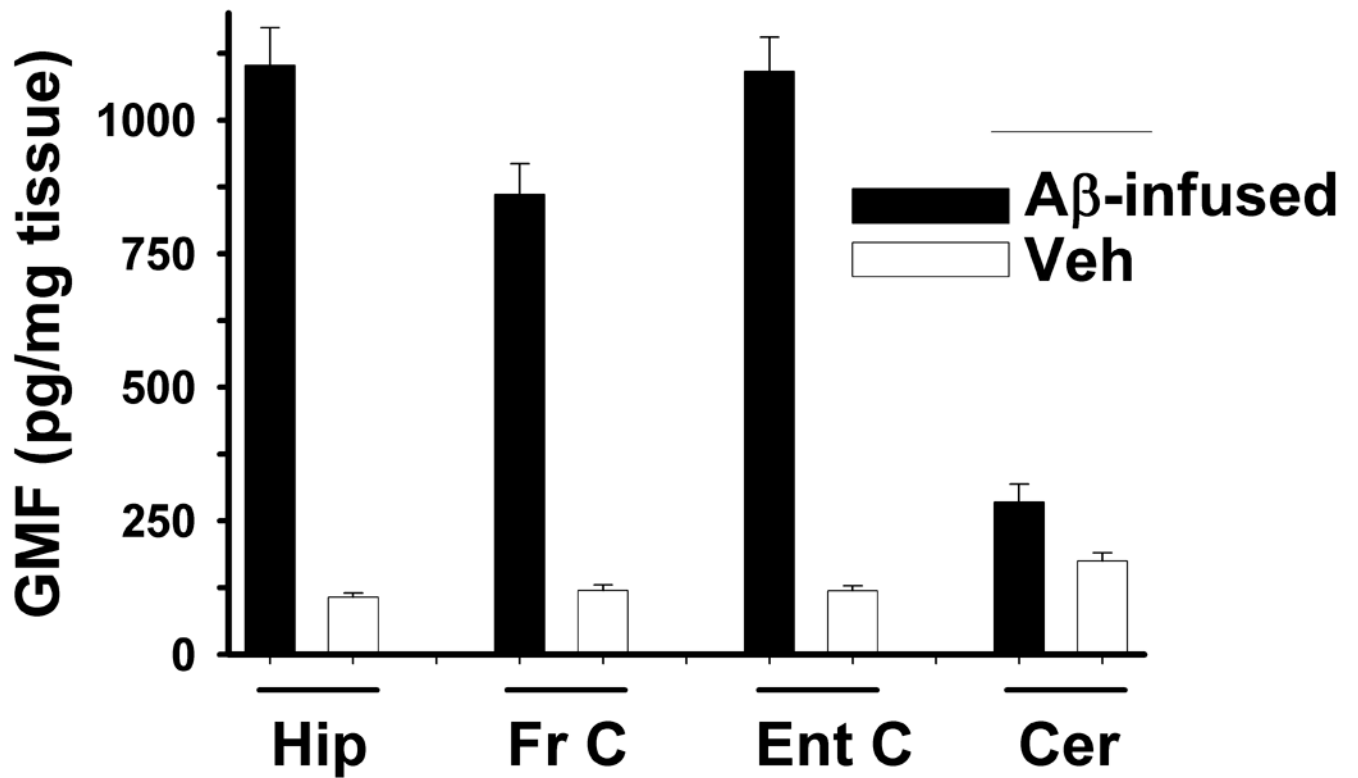
Fig. 8.
GMF levels are elevated in the hippocampus (Hip), frontal cortex (Fr C), entorhinal cortex (Ent C), and cerebellum (Cer) of Aβ1-42-infused mice compared to Veh-infused mice (via micro-pump for28 days). Quantitaive ELISA was performed as described in Methods. (n = 7/group).
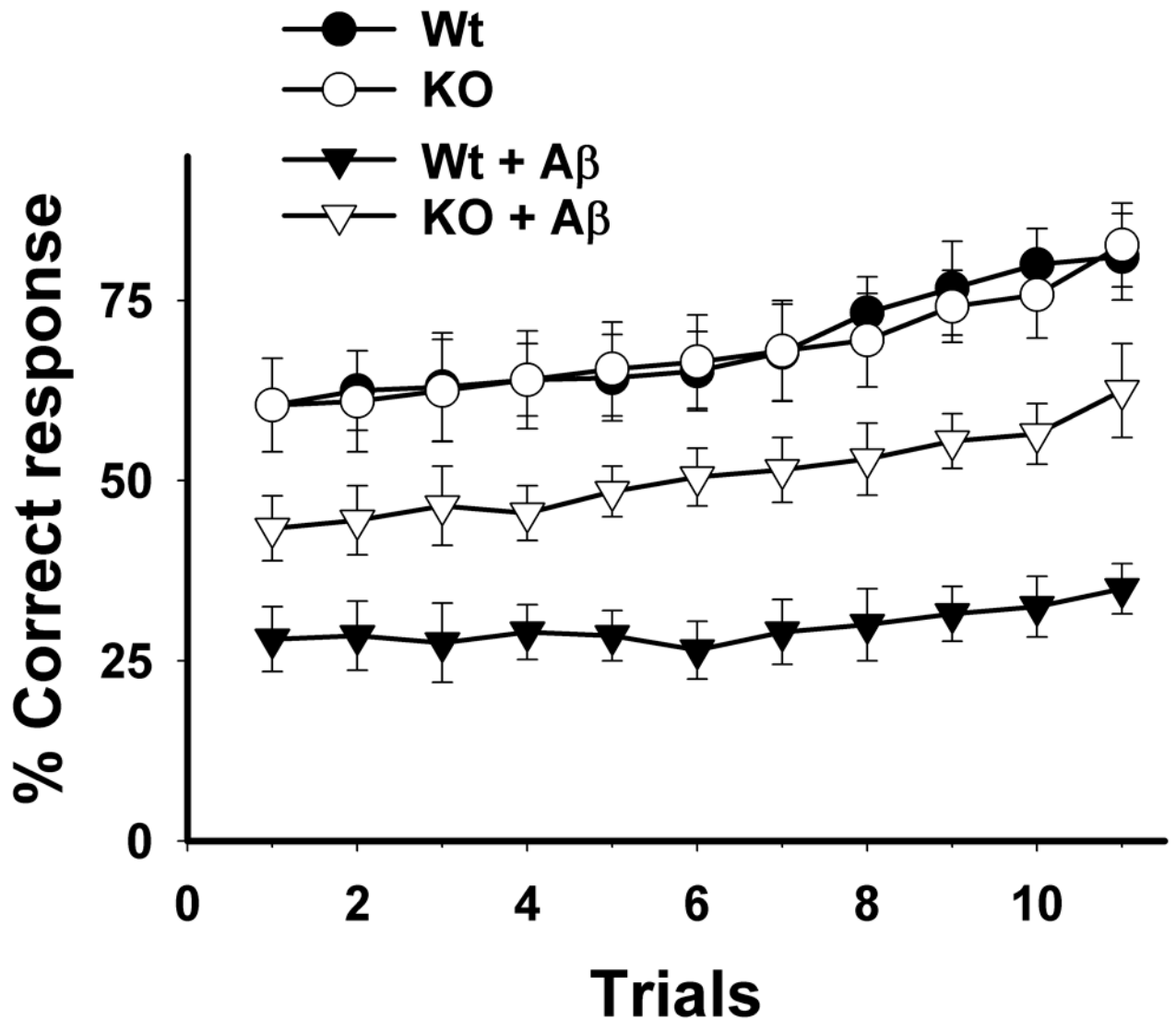
Fig. 9.
T-maze training for simple position discrimination, showing learning curves for Wt **(A)** and
GMF-KO **(B)** mice following vehicle and Aβ infusion (28 days). GMF-KO group consisted
of 12 mice, and the Wt group, 14 mice. Values are mean of each group for each day (±S.E.M.).
Logistic regression analysis using the method of generalized estimating equations (GEE) was
use to compare the mean % correct response between the two groups. The data for this analysis
was the number of correct responses out of 10 attempts repeated over 11 days. A logistic model
was employed because the outcome variable has a binomial distribution with the GEE method
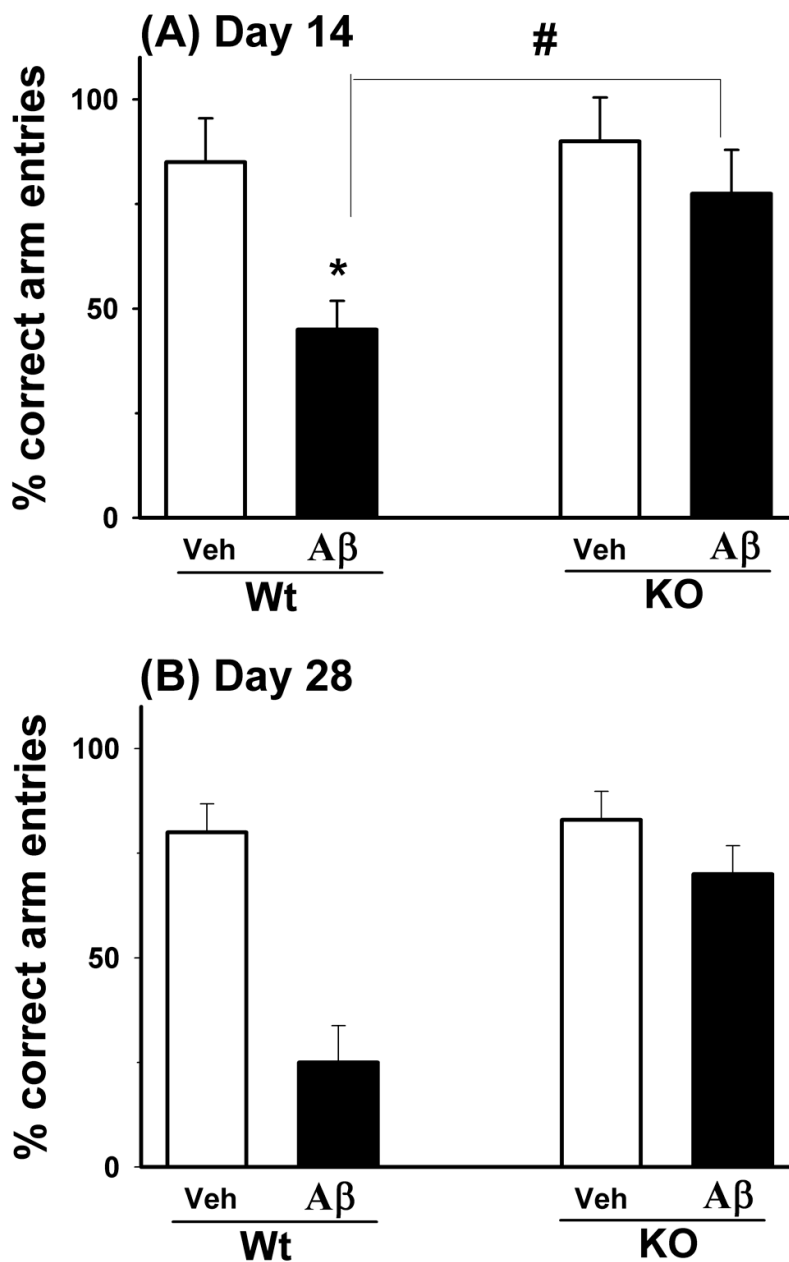used to account for the correlation of repeated measures from the same mouse.

Fig. 10.
Significantly improved memory retention in GMF-KO mice compared to Wt mice in the Y-maze test following Aβ infusion. Mice were trained in the Y maze for 5 days, with two sessions per day. The memory test was carried out in GMF-KO and Wt mice at **(A)** day 14 and **(B)** day 28 post Aβ 1-42 infusion, with the food placed in the same arm as it had been during the training. The data show the average percentage of mice that entered the correct arm per session of six trials ± SEM (n = 11). * Vehicle-infused Vs Aβ-infused. # Aβ-infused Wt Vs Aβ-infused GMF-KO. (p< 0.05)
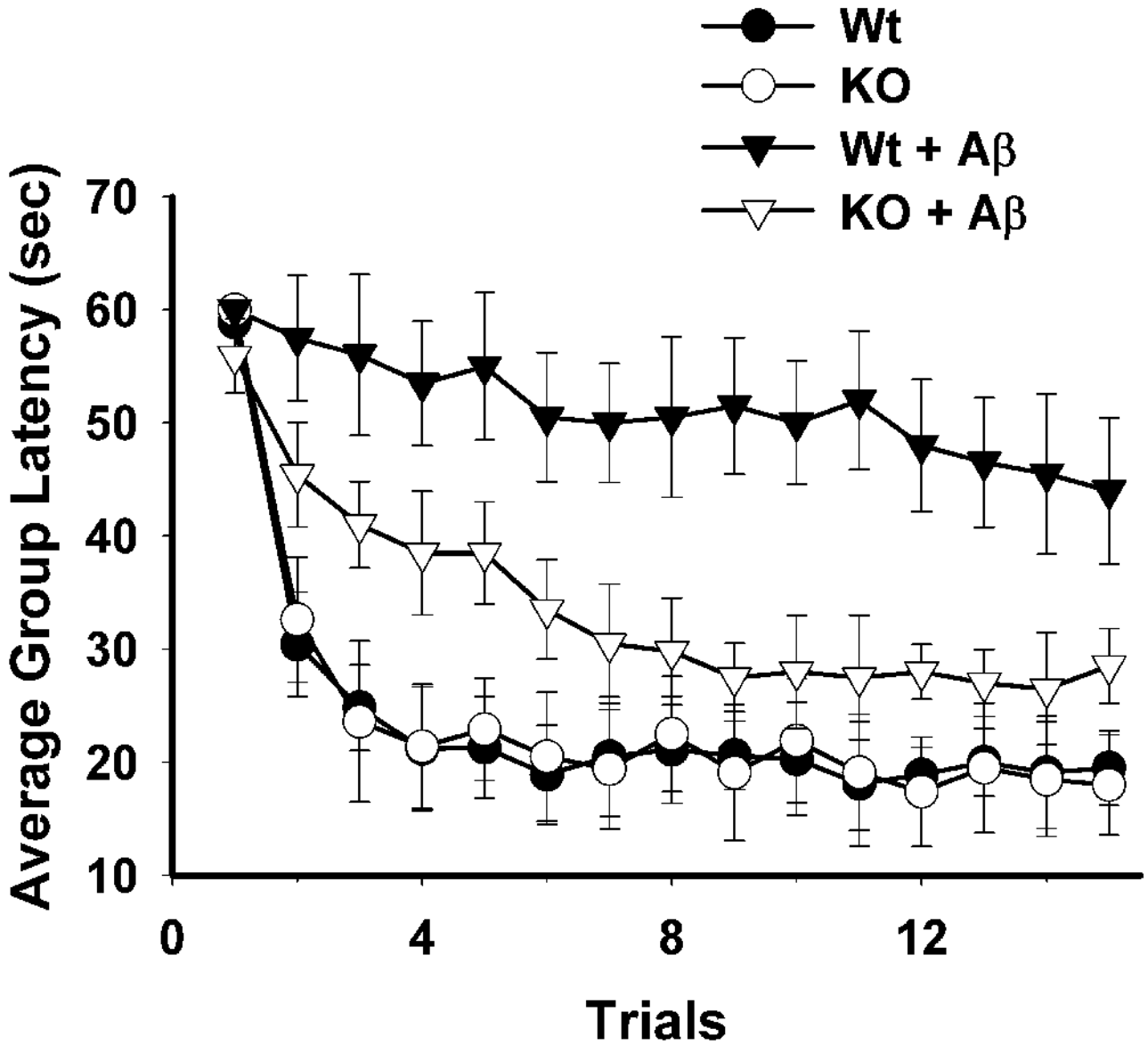
Fig. 11.
Morris water-maze training showing learning curves for GMF-KO and Wt mice. Ordinate is
the average time (in seconds) needed to locate the hidden platform. Error bars denote S.E.M.;
n=12 per group. The linear mixed model analysis for repeated measures was used to compare
mean latency between GMF-KO and the Wt mice over the conditioning period. The factors in
the model included group (KO vs. Wt), day (1 to 15), and group–day interaction. In addition,
since the starting location varied with location of the target platform (see Materials and
methods), starting location relative to the location of the target (opposite vs. same) was also
included as a factor in the model. (For example, when the target platform was SW, then a
starting location of N or E was labeled as opposite and S or W as same.) The natural log
transformation of the latency data was used in the analysis, as this was necessary to normalize
the data distribution. The results were subsequently replicated two times using different groups
of animals.